This article has been accepted for publication in IEEE Transactions on Vehicular Technology. This is the author's version which has not been fully edited and content may change prior to final publication. Citation information: DOI 10.1109/TVT.2023.3271874

Zero-Energy Device Networks with Wireless-Powered RISs

Yu Zheng, Sotiris A. Tegos, *Member, IEEE*, Yue Xiao, Panagiotis D. Diamantoulakis, *Senior Member, IEEE,* Zheng Ma, *Member, IEEE,* George K. Karagiannidis, *Fellow, IEEE*

***Abstract*—In order to realize massive connectivity, high spectral, and energy efficiency in future internet of things (IoT) networks, reconfigurable intelligent surfaces (RISs) are considered as a promising solution with their low cost and channel-adjusting ability. However, the ever-growing massive number of devices in RIS-empowered IoT networks requires achieving energy self-sustainability for the entire network. Motivated by this, a simultaneous wireless information and power transfer system empowered by a wireless-powered RIS has been investigated under the condition of imperfect channel state information, in which both the RIS and zero-energy devices (ZEDs) harvest energy with the power-splitting (PS) scheme for their operation. Specifically, a non-convex transmit power minimizing problem is formulated to handle the power-limited issue of practical IoT networks, where the PS ratios of the ZEDs, the active beamforming of the access point and RIS reflective coefficients are jointly optimized and solved by an efficient alternating optimization framework. The improved performance of the proposed algorithm against the benchmark schemes and its robustness are verified by simulation results, which highlight the effectiveness of the proposed algorithm in practical IoT networks.**

***Index Terms*—alternating optimization (AO) algorithm, imperfect channel state information (CSI), reconfigurable intelligent surface (RIS), simultaneous wireless information and power transfer (SWIPT).**

I. Introduction

FUTURE internet of things (IoT) networks are expected to provide more intelligent and reliable communication services for achieving massive connectivity, higher network coverage, larger network capacity, and low-cost deployment. To fulfill the increasing demands, the recently proposed reconfigurable intelligent surfaces (RISs), which operate as passive beamformers, have been considered as an appealing technology for achieving high spectral and energy efficiency in future IoT networks because of their low cost and channel-adjusting ability [1]. However, the massive use of IoT devices and RISs is challenging due to their requirement for energy supply, which implies either the connection of the nodes to the power grid or the frequent charging/replacement of batteries. For this purpose, the concept of zero-energy nodes, which from the user perspective operate without requiring access to the power grid, charging or battery replacement [2], would facilitate the massive use of IoT devices and RISs. It deserves to be noted that the energy independence of the devices which is achieved by using energy harvesting (EH) has been identified as a key challenge for the next-generation IoT [3].

For the realization of self-sustainable IoT networks, the power-splitting (PS) based simultaneous wireless information and power transfer (PS-SWIPT) technique, where the integrated PS-based devices are considered to split the power from the received radio frequency (RF) signal for both EH and information decoding (ID), has been regarded as a promising practical solution due to its characteristics of time-delay tolerance and robustness against coarse time synchronization. In [4], [5], the transmit power minimization problem with the PS-SWIPT scheme was studied to improve the performance in RIS-assisted networks, while, in [5], the power consumption of the active RIS was considered. Nevertheless, the power consumption of the passive RIS has not been investigated and is assumed to be negligible in the majority of research in this area [4], [6], [7]. Therefore, the integration of passive RISs and PS-SWIPT should be in-depth investigated considering the realistic non-negligible power consumption of the passive RISs.

In this direction, recently, the concept of wireless-powered RISs [8], also termed self-sustainable RISs, where the RIS performs information transmission (IT) and EH utilizing PS by adjusting its reflective coefficients, provides a new perspective for the realization of the self-sustainability of the networks [9]-[13]. In [9], self-sustainable RISs were utilized in wireless-powered communication networks (WPCNs), where the two-piece linear model was employed for EH. In [10], a self-sustainable RIS was utilized to enhance a wireless power transfer (WPT) system using an absorb-then-reflect scheme, while IT was not considered. Moreover, in [11], self-powered RISs were utilized in wireless-powered communication networks, where the harvest-then-transmit protocol was employed on the user side. In [12], the minimizing transmit power problem with a self-sustainable RIS was investigated aiming to enhance the performance of the wireless network. In [13], the sum-rate maximizing problem was investigated in a self-sustainable RIS-aided system, where information users and energy users are served separately.

In the existing literature, the use of SWIPT to achieve self-sustainability at both the RIS and zero-energy device (ZEDs) has not been considered or optimized. Therefore, in this work, we investigate a wireless-powered RIS-assisted network, where ZEDs utilize PS-SWIPT. The main contributions of this work are summarized as follows:

- We study a practical system aiming at self-sustainability at both the RIS and the devices, considering imperfect CSI and a non-linear EH model.
- We formulate a transmit power minimizing problem in

The work of Yu Zheng and Zheng Ma is supported by NSFC project U2268201 and 62271419. The work of Yue Xiao was supported by NSFC 62201477 and Sichuan Youth Fund Project 2023NSFSC1374. (Corresponding author: Yue Xiao.)

Y. Zheng, Y. Xiao, and Z. Ma are with the Provincial Key Lab of Information Coding and Transmission, Southwest Jiaotong University, Chengdu 611756, China (e-mails: zhengyu@my.swjtu.edu.cn; alice_xiaoyue@hotmail.com; zma@swjtu.cn).

S. A. Tegos, P. D. Diamantoulakis, and G. K. Karagiannidis are with the Electrical and Computer Engineering Department, Aristotle University of Thessaloniki, 54124 Thessaloniki, Greece. (e-mails: tegosoti@auth.gr; padiaman@auth.gr; geokarag@auth.gr). S. A. Tegos and P. D. Diamantoulakis are also with the Provincial Key Laboratory of Information Coding and Transmission, Southwest Jiaotong University, Chengdu 610031, China. G. K. Karagiannidis is also with the Cyber Security Systems and Applied AI Research Center, Lebanese American University (LAU), Lebanon.

This article has been accepted for publication in IEEE Transactions on Vehicular Technology. This is the author's version which has not been fully edited and content may change prior to final publication. Citation information: DOI 10.1109/TVT.2023.3271874

a multi-user multi-input single-output (MISO) system, where the active beamforming (ABF), the PS ratios of the ZEDs and each of the RIS elements, and the phase shifts of the RIS are jointly optimized.
- Unlike most works where either RIS reflective amplitude or phase shifts are considered, we jointly optimize these two parameters. Moreover, the considered practical non-linear EH model and the channel uncertainty improve the robustness of the proposed algorithm.
- To tackle the non-convexity of the formulated problem, we propose an efficient algorithm by using alternating optimization (AO) and semi-definite programming (SDP).
- Simulations demonstrate the performance of the proposed strategy highlighting the gains of optimizing the RIS reflective coefficients compared with benchmark schemes.

II. System Model and Problem Formulation

A. System Model

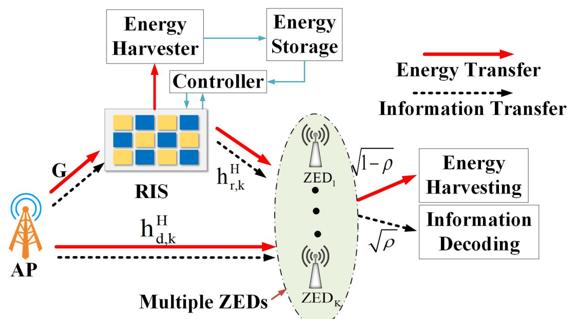

Fig. 1. Wireless-powered RIS-empowered PS-SWIPT system.

As shown in Fig. 1, we consider a single-cell downlink MISO PS-SWIPT system empowered by a wireless-powered RIS with N elements. The access point (AP) with M antennas serves K multiple single-antenna ZEDs. The wireless-powered RIS operates with the PS protocol, where the reflective coefficient is adjusted to meet both the ID and EH requirements of the RIS, thus a portion of the AP's power is fed into the RIS for EH and the remaining one is reflected by the RIS to enhance the received power at the ZEDs. Therefore, the RIS reflective coefficient is denoted by

$$\phi_n = \beta_n e^{j\theta_n}, \forall n, \tag{1}$$

where β_n and $\theta_n \in [0, 2\pi)$ are the reflective amplitude and phase shift of the n-th element, respectively. Moreover, the coefficient matrix of the RIS is given by $\mathbf{\Phi} = \mathrm{diag}\{\phi_1, \ldots, \phi_N\}$. The channels from the AP to the RIS, from the RIS to the k-th ZED, and from the AP to the k-th ZED are expressed as $\mathbf{G} \in \mathbb{C}^{N\times M}$, $\mathbf{h}^H_{r,k} \in \mathbb{C}^{1\times N}$ and $\mathbf{h}^H_{d,k} \in \mathbb{C}^{1\times M}$, respectively. Thus, the received signal at k-th ZED is expressed as

$$y_k = \mathbf{h}^H_k \sum_{i=1}^{K} \mathbf{w}_i s_i + n_k, \forall k, \tag{2}$$

where $n_k \sim \mathcal{CN}(0, \sigma^2_k)$ is the antenna noise vector at the k-th ZED, s_k represents the unit-power complex valued information symbol of k-th ZED, $\mathbf{w}_k \in \mathbb{C}^{M\times 1}$ denotes the corresponding beamforming vector and $\mathbf{h}^H_k = \mathbf{h}^H_{d,k} + \mathbf{h}^H_{r,k}\mathbf{\Phi}\mathbf{G}$ denotes the equivalent channel from the AP to the k-th ZED, whose CSI are assumed not to be perfectly obtained. Thus, we model the equivalent channel as $\mathbf{h}_k = \hat{\mathbf{h}}_k + \Delta\mathbf{h}_k$, $\forall k$, where $\hat{\mathbf{h}}_k$ denotes the acquired channel estimation and $\Delta\mathbf{h}_k$ is the estimation error with Gaussian distribution and zero mean, i.e., $\Delta\mathbf{h}_k \sim \mathcal{CN}(0, \sigma^2_{\Delta_k})$. We assume that the statistical information of $\Delta\mathbf{h}_k$ cannot be obtained, but a certain threshold can be obtained as $\|\Delta\mathbf{h}_k\| \le \epsilon_k, \forall k$ [14]. Accordingly, based on the assumption that $\mathbf{h}_k$ and $\Delta\mathbf{h}_k$ are independent of each other, the channel covariance matrix [7] is expressed as $\mathbf{H}_k = \hat{\mathbf{H}}_k + \Delta\mathbf{H}_k$, where $\mathbf{H}_k = \mathbb{E}\{\mathbf{h}_k\mathbf{h}^H_k\} \in \mathbb{C}^{M\times M}$, $\hat{\mathbf{H}}_k = \mathbb{E}\{\hat{\mathbf{h}}_k\hat{\mathbf{h}}^H_k\} \in \mathbb{C}^{M\times M}$, and $\Delta\mathbf{H}_k = \mathbb{E}\{\Delta\mathbf{h}_k\Delta\mathbf{h}^H_k\} \in \mathbb{C}^{M\times M}$ denote the real channel covariance matrix, the estimated equivalent channel covariance matrix, and the covariance uncertainty matrix of the equivalent channel, respectively, with $\mathbb{E}\{\cdot\}$ denoting expectation. Thus, the size of the covariance uncertainty matrix of the equivalent channel can be limited by a certain threshold as $\|\Delta\mathbf{H}_k\| \le \epsilon^2_k, \forall k$ [7], [14].

In this work, a PS protocol is adopted in the wireless-powered RIS, where the RIS reflective coefficients matrix $\mathbf{\Phi}$ is adjusted to meet the EH and IT requirement of the RIS. Thus, the received power by the RIS is

$$P_{\mathrm{in,RIS}} = \sum_{i=1}^{K} \mathrm{tr}\left(\mathbf{w}^H_i \mathbf{G}^H \mathbf{G} \mathbf{w}_i\right). \tag{3}$$

Moreover, utilizing (1), the RIS reflected power is given by

$$P_{\mathrm{out,RIS}} = \sum_{i=1}^{K} \mathrm{tr}\left(\mathbf{w}^H_i \mathbf{G}^H \mathbf{\Phi}^H \mathbf{\Phi} \mathbf{G} \mathbf{w}_i\right), \tag{4}$$

where $\|\mathbf{\Phi}\|$ cannot exceed 1 due to the use of the passive RIS. Therefore, the split power of the received signal at the RIS for EH is calculated as $P_{r,\mathrm{RIS}} = P_{\mathrm{in,RIS}} - P_{\mathrm{out,RIS}}$ [13], i.e.,

$$P_{r,\mathrm{RIS}} = \sum_{i=1}^{K} \mathrm{tr}\left(\mathbf{w}^H_i \mathbf{G}^H \left(\mathbf{I} - \mathbf{\Phi}^H \mathbf{\Phi}\right) \mathbf{G} \mathbf{w}_i\right). \tag{5}$$

It should be noted that, since the positions of the AP and RIS are usually deployed in advance, the channel from the AP to RIS $\mathbf{G}$ is assumed to be perfectly obtained.

The received signal power at each ZED is split into two portions by an adjustable PS ratio $\rho_k \in (0, 1)$, in which the ρ_k portion is used for ID operation and the $1 - \rho_k$ portion is for EH operation. The received signal at the k-th ZED for ID operation is expressed as

$$y_{k,\mathrm{ID}} = \sqrt{\rho_k}\left(\mathbf{h}^H_k \sum_{i=1}^{K} \mathbf{w}_i s_i + n_k\right) + z_k, \forall k, \tag{6}$$

where $z_k \sim \mathcal{CN}(0, \delta^2_k)$ is the additional noise generated during signal processing. Thus, the signal-to-interference plus noise ratio (SINR) at the k-th ZED is given by

$$\mathrm{SINR}_k = \frac{\rho_k \mathrm{tr}\left(\mathbf{w}^H_k(\mathbf{H}_k + \Delta\mathbf{H}_k)\mathbf{w}_k\right)}{\rho_k \sum_{i\ne k}^{K} \mathrm{tr}\left(\mathbf{w}^H_i(\mathbf{H}_k + \Delta\mathbf{H}_k)\mathbf{w}_i\right) + \rho_k\sigma^2_k + \delta^2_k}, \forall k. \tag{7}$$

Accordingly, the received signal of the k-th ZED for EH operation is given by

$$y_{k,\mathrm{EH}} = \sqrt{1-\rho_k}\left(\mathbf{h}^H_k \sum_{i=1}^{K} \mathbf{w}_i s_i + n_k\right), \forall k. \tag{8}$$

In EH, differently to ID, by ignoring the antenna noise power, i.e., σ^2_k, which is negligible compared with the harvesting power [5], the split power of the received signal at the k-th ZED for EH can be expressed as

$$P_{r,k} = (1-\rho_k)\sum_{i=1}^{K} \mathrm{tr}\left(\mathbf{w}^H_i\left(\mathbf{H}_k + \Delta\mathbf{H}_k\right)\mathbf{w}_i\right), \forall k. \tag{9}$$

Regarding EH, we employ a general and practical logistic function-based non-linear model [7], which is modeled as

$$\Psi_0(x) = \frac{\psi_{\max}}{X(1+\exp(-a_{\mathrm{eh}}(x - b_{\mathrm{eh}})))} - Y, \tag{10}$$

where x represents the corresponding received power, $\psi_{\max}$ is the maximum harvested power when the circuit is saturated, a_{eh} and b_{eh} are constants related to specific circuit specifications, $X = \frac{\exp(a_{\text{eh}} b_{\text{eh}})}{1+\exp(a_{\text{eh}} b_{\text{eh}})}$, and $Y = \frac{\psi_{\max}}{\exp(a_{\text{eh}} b_{\text{eh}})}$. Hence, the inverse function of $\Psi_0(P_r)$ is given by

$$\Psi_0^{-1}(x) = b_{\text{eh}} - \frac{1}{a_{\text{eh}}} \ln\left(\frac{\psi_{\max}}{(x+Y)X} - 1\right). \tag{11}$$

Moreover, $P_{\min,\text{k}}$ denotes the required power requirement of the k-th ZED, while considering that the circuit power consumption of each RIS element is μ, the total power requirement of the RIS is given by $N\mu$ [12]. Therefore, the harvested power of the k-th ZED and the RIS should be greater than or equal to $P_{\min,\text{k}}$ and $N\mu$, respectively, and the constraints of the power consumption at the k-th ZED and the RIS are given, respectively, by

$$P_{r,k} \geq \Psi_0^{-1}(P_{\min,k}), \forall k, \tag{12}$$

$$P_{r,\text{RIS}} \geq \Psi_0^{-1}(N\mu). \tag{13}$$

B. Problem Formulation

Let $\boldsymbol{\rho} = [\rho_1, \ldots, \rho_K] \in \mathbb{R}^{1\times K}$ and $\mathbf{W} = [\mathbf{w}_1, \ldots, \mathbf{w}_K] \in \mathbb{C}^{M\times K}$. In this paper, we aim to minimize the transmit power at the AP by jointly optimizing the PS ratio, the ABF at the AP and the RIS reflective coefficients, thus the problem is formulated as

$$\begin{aligned}
\min_{\boldsymbol{\Phi}, \mathbf{W}, \boldsymbol{\rho}} \quad & \sum_{k=1}^{K} |\mathbf{w}_k|^2 \qquad \text{(P1)}\\
\text{s.t.} \quad & C1: \text{SINR}_k \geq \gamma_k, \forall k,\\
& C2: P_{r,k} \geq \Psi_0^{-1}(P_{\min,k}), \forall k,\\
& C3: \|\Delta\mathbf{H}_k\| \leq \epsilon_k^2, \forall k,\\
& C4: P_{r,\text{RIS}} \geq \Psi_0^{-1}(N\mu),\\
& C5: |\phi_n| \leq 1, n = 1, \ldots, N,\\
& C6: 0 \leq \rho_k \leq 1, \forall k,
\end{aligned}$$

where $\gamma_k > 0$ is the minimum SINR requirement of the k-th ZED. Although the objective function of (P1) and constraints $C3$, $C5$, $C6$ are convex, it is challenging to solve (P1) due to the non-convex constraints $C1$, $C2$, $C4$ and coupled variables. In general, there is no standard method for solving such non-convex optimization problems optimally. Moreover, to ensure that the formulated problem is feasible, we present the following lemma.

Lemma 1: *For the considered non-linear EH model, to ensure that the RIS can harvest enough power for its operation, the maximum number of the RIS should satisfy*

$$N_{\max} \leq {}^{\psi_{\max}}/_{\mu}. \tag{14}$$

Proof: In order the self-sustainable RIS to assist in the downlink SWIPT system, we must have $N\mu \leq \psi_{\max}$ for the non-linear EH model. Otherwise, if $N\mu > \psi_{\max}$, the RIS cannot harvest enough energy to power itself. Thus, (14) *is derived, which concludes the proof.* ∎

In the next section, we investigate the problem (P1) when the condition (14) is satisfied.

III. Alternating Optimization Framework

In this section, we propose an AO-based framework to solve the non-convex optimization problem, where the original problem is divided into three sub-problems and each variable is optimized iteratively with others fixed until the convergence is achieved. To handle the problem, we first transform constraints according to **Lemma 2** in [7], which is presented below.

Lemma 2: For any given Hermitian matrixes $\mathbf{A}$ and $\mathbf{B}$, if $\mathbf{B}$ satisfies $\|\mathbf{B}\| \leq \epsilon^2$, then

$$\max_{\|\mathbf{B}\|\leq\epsilon^2} \text{tr}(\mathbf{AB}) = \epsilon^2 \|\mathbf{A}\|_* = \epsilon^2 \text{tr}(\mathbf{A}) \tag{15}$$

holds, where $\|\mathbf{A}\|_*$ denotes the dual norm of matrix A.

Proof: The detailed proof is provided in [7]. ∎

Then, using $\mathbf{w}_k^H \Delta\mathbf{H}_k \mathbf{w}_k = \text{tr}\left(\Delta\mathbf{H}_k \mathbf{w}_k \mathbf{w}_k^H\right) = \text{tr}\left(\Delta\mathbf{H}_k \mathbf{W}_k\right)$, where $\mathbf{W}_k = \mathbf{w}_k \mathbf{w}_k^H \succeq 0$ and $\text{rank}(\mathbf{W}_k) = 1$. Based on Lemma 1, we have

$$\max_{\|\Delta\mathbf{H}_k\|\leq\epsilon_k^2} \text{tr}(\Delta\mathbf{H}_k \mathbf{W}_k) = \epsilon_k^2 \|\mathbf{W}_k\|_* = \epsilon_k^2 \text{tr}(\mathbf{W}_k) \tag{16}$$

In the worst case, i.e., to satisfy the minimal user's SINR and EH requirements in the worst channel condition, the AP needs to transmit the power to compensate the maximum CSI error threshold [7]. Thus, $\Delta\mathbf{H}_k$ in the denominator of $C1$ needs to reach its maximum as $\epsilon_k^2\mathbf{I}$, while in the numerator of $C1$ and in $C2$, it should reach its minimum as $-\epsilon_k^2\mathbf{I}$, by which the worst channel condition is satisfied.

To this end, based on $C3$ and **Lemma 2**, $C1$ and $C2$ can be rewritten, respectively, as

$$C7: \text{SINR}_k = \frac{\rho_k \text{tr}\left((\mathbf{H}_k - \epsilon_k^2\mathbf{I})\mathbf{W}_k\right)}{\rho_k \sum_{i\neq k}^{K} \text{tr}((\mathbf{H}_k + \epsilon_k^2\mathbf{I})\mathbf{W}_i) + \rho_k\sigma_k^2 + \delta_k^2} \geq \gamma_k, \forall k,$$

$$C8: P_{r,k} = (1-\rho_k)\sum_{i=1}^{K} \text{tr}((\mathbf{H}_k - \epsilon_k^2\mathbf{I})\mathbf{W}_i) \geq \Psi_0^{-1}(P_{\min,k}), \forall k.$$

Therefore, the original problem (P1) can be transformed into the problem (P2) as

$$\begin{aligned}
\min_{\boldsymbol{\Phi}, \mathbf{W}, \boldsymbol{\rho}} \quad & \sum_{k=1}^{K} |\mathbf{w}_k|^2 \qquad \text{(P2)}\\
\text{s.t.} \quad & C4 - C8.
\end{aligned}$$

A. Joint optimization at the AP and ZED side

Firstly, with given $\boldsymbol{\Phi}$, the sub-problem of joint optimizing ABF $\mathbf{W}$ and PS ratio $\boldsymbol{\rho}$ can be formulated as

$$\begin{aligned}
\min_{\mathbf{W}, \boldsymbol{\rho}} \quad & \sum_{k=1}^{K} |\mathbf{w}_k|^2 \qquad \text{(P3)}\\
\text{s.t.} \quad & C4,\ C7,\ C8.
\end{aligned}$$

Problem (P3) is similar to the power minimization problem in the multi-user MISO downlink SWIPT system [5], which is regarded as an SDP problem by omitting the rank-one constraint, i.e., $\textbf{Rank}\,(\mathbf{W}_k) \leq 1$, and is solved by CVX [15].

B. Optimization at the RIS Side

Finally, we consider the optimization at the RIS side. By utilizing the obtained solutions for $\boldsymbol{\rho}$ and $\mathbf{W}$, we need to optimize the RIS reflective coefficients $\boldsymbol{\phi} = [\phi_1, \ldots, \phi_N]$. Obviously, this sub-problem is still non-convex, because the variables are coupled in the constraints. To make it tractable, we set $\mathbf{h}_{d,k}^H \mathbf{w_i} = b_{k,i}$, $\mathbf{a}_{k,i} = \text{diag}(\mathbf{h}_{r,k}^H)\mathbf{G}\mathbf{w}_i$ and we have $\mathbf{h}_{r,k}^H \boldsymbol{\Phi}\mathbf{G}\mathbf{w}_i = \boldsymbol{\phi}\mathbf{a}_{k,i}$. Similarly, we set $\mathbf{c}_i = \mathbf{G}\mathbf{w}_i$ so that $\mathbf{w}_i^H \mathbf{G}^H \boldsymbol{\Phi}^H \boldsymbol{\Phi}\mathbf{G}\mathbf{w}_i = \mathbf{c}_i^H \boldsymbol{\phi}^H \boldsymbol{\phi}\mathbf{c}_i$, and $\mathbf{v} = [\boldsymbol{\phi}, l]^T$ with l being an auxiliary variable so that $\mathbf{V} = \mathbf{v}\mathbf{v}^H$, where $\mathbf{V} \succeq 0$ and $\text{rank}(\mathbf{V}) = 1$. Based on the above, the constraints $C4$, $C7$ and $C8$ can be rewritten, respectively, as

$$
\begin{aligned}
C9: P_{r,\mathrm{RIS}} &= \sum_{i=1}^{K} \mathrm{tr}\left(\mathbf{w}_i^H \mathbf{G}^H \left(\mathbf{I} - \mathbf{\Phi}^H \mathbf{\Phi}\right) \mathbf{G} \mathbf{w}_i\right) \\
&= \sum_{i=1}^{K} \mathrm{tr}\left(\mathbf{R}_i^{'}\right) - \sum_{i=1}^{K} \mathrm{tr}\left(\mathbf{R}_i^{'} \mathbf{V}\right) \geq \Psi_0^{-1}(N\mu),
\end{aligned}
$$

$$
\begin{aligned}
C10: \mathrm{tr}(\mathbf{R}_{k,k}\mathbf{V}) + |b_{k,k}|^2 \geq \gamma_k \sum_{i\neq k}^{K} \mathrm{tr}(\mathbf{R}_{k,i}\mathbf{V}) + \epsilon_k^2 \mathrm{tr}(\mathbf{W}_k) \\
+ \gamma_k \epsilon_k^2 \sum_{i\neq k}^{K} \mathrm{tr}(\mathbf{W}_i) + \gamma_k \left(\sum_{i\neq k}^{K} |b_{k,i}|^2 + \sigma_k^2 + \frac{\delta_k^2}{\rho_k} \right), \forall k,
\end{aligned}
$$

$$
\begin{aligned}
C11: &\sum_{i=1}^{K} \mathrm{tr}(\mathbf{R}_{k,i}\mathbf{V}) + \sum_{i=1}^{K} |b_{k,i}|^2 - \epsilon_k^2 \sum_{i=1}^{K} \mathrm{tr}(\mathbf{W}_i) \\
&\geq \frac{\Psi_0^{-1}(P_{\min,k})}{(1-\rho_k)}, \forall k,
\end{aligned}
$$

where $\mathbf{R}_{k,i} = \begin{bmatrix} \mathbf{a}_{k,i}\mathbf{a}_{k,i}^H & \mathbf{a}_{k,i} b_{k,i}^H \\ \mathbf{a}_{k,i}^H b_{k,i} & 0 \end{bmatrix}$, $\mathbf{R}_i^{'} = \begin{bmatrix} \mathbf{c}_i \mathbf{c}_i^H & 0 \\ 0 & 0 \end{bmatrix}$.

To this end, the sub-problem in the RIS side is written as

$$
\begin{aligned}
\min_{\mathbf{V}} \; & \sum_{k=1}^{K} |\mathbf{w}_k|^2 \qquad \text{(P4)} \\
\text{s.t. } & C9,\ C10,\ C11, \\
& C12: \mathbf{V} \succeq 0, \\
& C13: \mathbf{V}_{n,n} \leq 1, \forall n, \\
& C14: \mathrm{rank}(\mathbf{V}) = 1.
\end{aligned}
$$

It should be highlighted that, by applying semidefinite relaxation, (P4) can be regarded as a convex SDP problem by relaxing the rank-one constraint $C14$, which can be optimally solved by using a standard convex optimization method. However, the solution obtained for the relaxed version may not guarantee the rank-one constraint. The Gaussian randomization method is then employed to construct a suboptimal rank-one solution to tackle this issue. The details of the process is similar with [9] and, thus, omitted here.

C. Computational Complexity and Convergence Analysis

Algorithm 1 describes the process of solving the proposed transmit power minimizing problem, where all variables are optimized in an alternating manner until convergence.

1) Computational Complexity Analysis: In each iteration, (P3) jointly optimizes the ABF and PS ratio and (P4) optimizes the RIS coefficients by solving and a relaxed SDP problem. Thus, the computational complexity of using the interior point method to solve (P3) and (P4) is $\mathcal{O}(K^{3.5}M^{2.5} + K^{2.5}M^{3.5})$ [5] and $\mathcal{O}(K(N+1)^{3.5})$, respectively [16]. Letting t present the number of iterations required for convergence, the overall computational complexity of the proposed AO algorithm can be expressed as $\mathcal{O}(tK(K^{2.5}M^{2.5} + K^{1.5}M^{3.5} + (N+1)^{3.5}))$.

2) Convergence Analysis: Let $\{\boldsymbol{\rho}^{(t)}, \mathbf{W}^{(t)}\}$ and $\mathbf{\Phi}^{(t)}$ represent the t-th solution of (P3) and (P4), respectively. The objective function of the proposed AO algorithm is expressed as $F(\boldsymbol{\rho}^{(t)}, \mathbf{W}^{(t)}, \mathbf{\Phi}^{(t)})$, thus we have the following inequalities

$$
\begin{aligned}
F(\boldsymbol{\rho}^{(t-1)}, \mathbf{W}^{(t-1)}, \mathbf{\Phi}^{(t-1)}) &\overset{(a_f)}{\leq} F(\boldsymbol{\rho}^{(t)}, \mathbf{W}^{(t)}, \mathbf{\Phi}^{(t-1)}) \\
&\overset{(b_f)}{\leq} F(\boldsymbol{\rho}^{(t)}, \mathbf{W}^{(t)}, \mathbf{\Phi}^{(t)}),
\end{aligned} \tag{17}
$$

where the inequalities (a_f) and (b_f) hold, since the values of $\{\boldsymbol{\rho}, \mathbf{W}\}$ and $\mathbf{\Phi}$ have been optimally determined sequentially when others are fixed. Therefore, since the objective function is non-increasing after each iteration, the convergence of **Algorithm 1** is guaranteed.

Algorithm 1 AO-based algorithm for solving P1

1: Initialize: Set $\{\boldsymbol{\rho}^{(0)}, \mathbf{W}^{(0)}, \mathbf{\Phi}^{(0)}\}$, and $t = 1$.
2: **repeat**
3: Given $\mathbf{\Phi}^{(t-1)}$, obtain the ABF and PS ratio $\{\boldsymbol{\rho}^{(t)}, \mathbf{W}^{(t)}\}$ based on (P3);
4: Given $\{\boldsymbol{\rho}^{(t)}, \mathbf{W}^{(t)}\}$, obtain the RIS reflective coefficients $\mathbf{\Phi}^{t}$ based on (P4);
5: Update the iterative number $t = t + 1$;
6: **until** Convergence.

IV. Simulation Results

In this section, numerical results and simulations are provided to evaluate the performance of the proposed AO-based algorithm. The coordinates of the AP with $M = 6$ antennas and the RIS with $N = 30$ elements are set as $(0, 0)$ and $(8, 2)$ in meters, respectively, while $K = 4$ ZEDs are randomly deployed within a circular area centered at $(8, 0)$ with radius 1 m. The channels G, $h_{r,k}$, $h_{d,k}$ are modeled as Rician fading with Rician factor 5. The large-scale path loss is given by $-30 - \alpha \log_{10}(d)$ dB, where d and α denote the distance and the path loss exponent of each link, respectively. We set the path loss factors of all channels as $\alpha_{d,k} = 3.6$, $\alpha_G = \alpha_{r,k} = 2.2$. In order to measure the relative amount of CSI uncertainties, the CSI error bounds are defined as $\epsilon_k = \xi \|\mathbf{h}_k\|$, i.e., $\epsilon_k^2 = \xi^2 \|\mathbf{H}_k\|$, where $\xi \in [0, 1)$ [14]. In the following simulation, ξ is set as 0.02. Other parameters for the simulation are given as follows: $\psi_{\max} = 84$ mW, $a_{\mathrm{eh}} = 150$, $b_{\mathrm{eh}} = 0.024$ $\sigma_k^2 = -100$ dBm, $\delta_k^2 = -50$ dBm, $\mu = 1$ mW, $P_{\min} = P_{\min,k} = 20$ mW, $\gamma_k = 20$ dB. For the sake of comparison, four benchmark schemes are adopted in the simulations, which are presented as, **benchmark (1)**: a system without a RIS, **benchmark (2)**: a similar system with a RIS with random phase shifts, **benchmark (3)**: a similar system with a two-piece linear EH model [9], where EH efficiency $\eta = 0.8$, and **benchmark (4)**: a similar system with an ideal RIS without power consumption are utilized as benchmarks.

To begin with, the convergence of the proposed algorithm is investigated in Fig. 2. Since **benchmark (1)** and **benchmark (2)** lack the sub-problem of optimizing the RIS reflective coefficient (P4), they cannot be compared with the proposed algorithm. Thus, only **benchmark (3)** and **benchmark (4)** are adopted for the comparison of the convergence. As shown, the proposed algorithm and benchmarks have converged in around 15 iterations, in which the proposed algorithm achieves a better performance than **benchmark (3)** while performing the same trend of convergence with **benchmark (3)** and **benchmark (4)**. This is explained considering that the **benchmark (3)** and **benchmark (4)** are special cases of the system where the two-piece linear EH model is adopted and the power consumption of the RIS element is set as $\mu = 0$, respectively. Conclusively, the different EH models and the different parameter settings of μ have no effect on the convergence of the algorithm, which highlights the robustness of the proposed algorithm.

This article has been accepted for publication in IEEE Transactions on Vehicular Technology. This is the author's version which has not been fully edited and content may change prior to final publication. Citation information: DOI 10.1109/TVT.2023.3271874

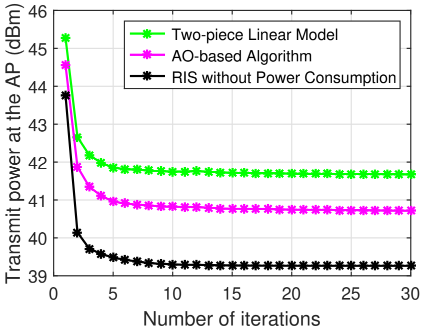

Fig. 2. AP transmit power versus the number of iterations.

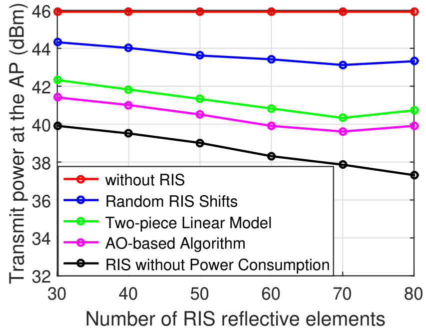

Fig. 3. AP transmit power versus number of RIS reflecting elements.

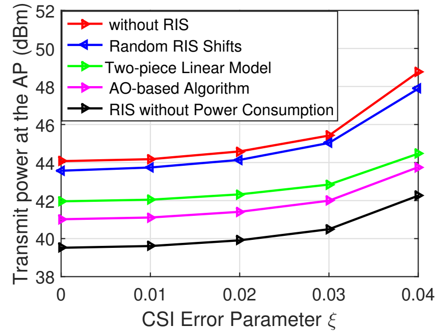

Fig. 4. AP transmit power versus CSI error parameter ξ.

In Fig. 3, the impact of the number of RIS reflective elements on AP transmit power is investigated. As shown, **benchmark (2)** outperforms **benchmark (1)**, which implies that the performance is enhanced by applying a RIS. Moreover, the proposed algorithm needs less transmit power than **benchmark (3)**, which implies the logistic function-based non-linear model outperforms the two-piece linear model. Furthermore, the theoretical maximum number of RIS elements is calculated as 70 in the proposed scheme, **benchmark (2)** and **benchmark (3)**, because of the trade-off between the increased power consumption and the improved performance that the increase of the number of RIS elements offers [9], [12], [13]. While this trade-off does not occur in the **benchmark (1)** and **benchmark (4)**, as expected. Specifically, the performance gain is firstly acquired by the additional channel links created by the increase of the number of the RIS, however, after the number of RIS elements exceeds the optimal value, the additional channel gain cannot compensate the gradually increasing circuit power consumption of the RIS. Thus, the number of RIS reflective elements should be carefully chosen for the optimal performance gain in practical implementation.

In Fig. 4, we depict the AP transmit power versus the CSI error parameter ξ. It can be observed that, as expected, the AP transmit power increases under all schemes, as the CSI error parameter ξ increases. This is because we aim to meet the users' SINR requirements and EH requirements in the worst channel condition [7]. Therefore, as the channel error increases, this negative effect should be compensated by increasing the AP transmit power. Moreover, perfect CSI is almost impossible to be obtained in practical systems, thus the proposed algorithm achieves better robustness and is more suitable for practical implementation.

V. Conclusion

In this paper, we have investigated a wireless-powered RIS-empowered PS-SWIPT system for handling energy-limited issues in practical IoT networks. Specifically, the transmit power minimizing problem with joint optimization of the PS ratios, the ABF and the RIS reflective coefficients has been studied. To tackle this non-convex problem, we have proposed an AO-based joint optimization framework, where the original problem with coupled variables has been decomposed into several sub-problems. In this direction, near-optimal solutions have been obtained in several iterations of the proposed algorithm. Moreover, simulation results have been performed to prove the superiority of our proposed algorithm in practical implementations in terms of performance and robustness compared with benchmark schemes. In the future scope, achieving self-sustainability for the network with different SWIPT schemes in more complicated scenarios considering multiple access schemes can be investigated.

References

[1] M. Di Renzo et al., "Smart Radio Environments Empowered by Reconfigurable Intelligent Surfaces: How It Works, State of Research, and The Road Ahead," *IEEE J. Sel. Areas Commun.*, vol. 38, no. 11, pp. 2450-2525, Nov. 2020.

[2] J. Hu, Q. Wang and K. Yang, "Energy Self-Sustainability in Full-Spectrum 6G," *IEEE Wireless Commun.*, vol. 28, no. 1, pp. 104-111, Feb. 2021.

[3] A. Brékine et al., "Building a Roadmap for the Next Generation Internet of Things. Research, Innovation and Implementation 2021 – 2027," *Scoping Paper*, Sep. 2019.

[4] Shayan Zargari, Shahrokh Farahmand, Bahman Abolhassani, "Joint design of transmit beamforming, IRS platform, and power splitting SWIPT receivers for downlink cellular multiuser MISO, Physical Communication," *Physical Communication*, vol. 48, Oct. 2021.

[5] S. Zargari, A. Hakimi, C. Tellambura and S. Herath, "Multiuser MISO PS-SWIPT Systems: Active or Passive RIS?," *IEEE Wireless Commun. Lett.*, vol. 11, no. 9, pp. 1920-1924, Sep. 2022.

[6] B. Zhang, K. Yang, K. Wang and G. Zhang, "Performance Analysis of RIS-Assisted Wireless Communications With Energy Harvesting," *IEEE Trans. Veh. Technol.*, vol. 72, no. 1, pp. 1325-1330, Jan. 2023.

[7] Z. Li, W. Chen, Q. Wu, H. Cao, K. Wang and J. Li, "Robust Beamforming Design and Time Allocation for IRS-Assisted Wireless Powered Communication Networks," *IEEE Trans. Commun.*, vol. 70, no. 4, pp. 2838-2852, Apr. 2022.

[8] K. Li, Y. Naderi, U. Muncuk and K. R. Chowdhury, "iSurface: Self-Powered Reconfigurable Intelligent Surfaces with Wireless Power Transfer," *IEEE Commun. Mag.*, vol. 59, no. 11, pp. 109-115, Nov. 2021.

[9] B. Lyu, P. Ramezani, D. T. Hoang, S. Gong, Z. Yang and A. Jamalipour, "Optimized Energy and Information Relaying in Self-Sustainable IRS-Empowered WPCN," *IEEE Trans. Commun.*, vol. 69, no. 1, pp. 619-633, Jan. 2021.

[10] Y. Cheng, W. Peng and T. Jiang, "Self-sustainable RIS Aided Wireless Power Transfer Scheme," *IEEE Trans. Veh. Technol.*, vol. 72, no. 1, pp. 881-892, Jan. 2023.

[11] H. Xie, B. Gu, D. Li, Z. Lin, Y. Xu, "Gain without Pain: Recycling Reflected Energy from Wireless Powered RIS-aided Communications," Available Online: https://arxiv.org/pdf/2209.13100.pdf, Sep. 2022.

[12] Y. Zou et al., "Robust Beamforming Optimization for Self-Sustainable Intelligent Reflecting Surface Assisted Wireless Networks," *IEEE Trans. Cogn. Commun. and Netw.*, vol. 8, no. 2, pp. 856-870, Jun. 2022.

[13] Y. Pan, K. Wang, C. Pan, H. Zhu and J. Wang, "Self-Sustainable Reconfigurable Intelligent Surface Aided Simultaneous Terahertz Information and Power Transfer (STIPT)," *IEEE Trans. Wireless Commun.*, vol. 21, no. 7, pp. 5420-5434, Jul. 2022.

[14] G. Zhou, C. Pan, H. Ren, K. Wang, M. D. Renzo and A. Nallanathan, "Robust Beamforming Design for Intelligent Reflecting Surface Aided MISO Communication Systems," *IEEE Wireless Commun. Lett.*, vol. 9, no. 10, pp. 1658-1662, Oct. 2020.

[15] M. Grant and S. Boyd, "CVX: MATLAB software for disciplined convex programming," 2016. [Online] Available: http: //cvxr.com/cvx.

[16] A. Ben-Tal and A. Nemirovski, Lectures on Modern Convex Optimization: Analysis, Algorithms, and Engineering Applications. Philadelphia, PA, USA: SIAM, 2001.